

Dissolution Kinetics of Macronutrient Fertilizers Coated with Manufactured Zinc Oxide Nanoparticles

Narges Milani,^{*,†} Mike J. McLaughlin,^{†,‡} Samuel P. Stacey,[†] Jason K. Kirby,[‡] Ganga M. Hettiarachchi,^{‡,§} Douglas G. Beak,^{‡,||} and Geert Cornelis^{†,⊥}

[†]Soil Science, School of Agriculture, Food and Wine, The University of Adelaide, PMB 1, Glen Osmond, South Australia 5064, Australia

[‡]Nanosafety, Advanced Materials Transformational Capability Platform, Environmental Biogeochemistry Program, CSIRO Land and Water, Waite Campus, Waite Road, Glen Osmond, South Australia 5064, Australia

[§]Department of Agronomy, Trockmorton Plant Sciences Centre, Kansas State University, Manhattan, Kansas 66506, United States

S Supporting Information

ABSTRACT: The solubility of Zn in Zn fertilizers plays an important role in the agronomic effectiveness of the fertilizer. On the basis of thermodynamics, zinc oxide (ZnO) nanoparticles (NPs) should dissolve faster and to a greater extent than bulk ZnO particles (equivalent spherical diameter >100 nm). These novel solubility features of ZnO NPs might be exploited to improve the efficiency of Zn fertilizers. In this study, we compared the Zn solubility and dissolution kinetics of ZnO nanoparticles and bulk ZnO particles coated onto two selected granular macronutrient fertilizers, urea and monoammonium phosphate (MAP). The main Zn species on coated MAP and urea granules were zinc ammonium phosphate and ZnO, respectively. Coated MAP granules showed greater Zn solubility and faster dissolution rates in sand columns compared to coated urea granules, which may be related to pH differences in the solution surrounding the fertilizer granules. The kinetics of Zn dissolution was not affected by the size of the ZnO particles applied for coating of either fertilizer type, possibly because solubility was controlled by formation of the same compounds irrespective of the size of the original ZnO particles used for coating.

KEYWORDS: zinc, ZnO, nanoparticles, solubility, dissolution kinetics, fertilizer

■ INTRODUCTION

Zinc deficiency is one of the most widely distributed micronutrient problems limiting agricultural productivity, with approximately 49% of the arable soils of the world being Zn deficient.^{1,2} Typically, solid Zn fertilizers are blended with, incorporated into, or coated onto macronutrient fertilizer to maintain a more uniform distribution of Zn in the field and to provide a cost-effective delivery of the small amounts of Zn required. The effectiveness of Zn fertilizers for providing plants with Zn in Zn-deficient soils mainly depends on the solubility of the Zn source in soil. Mortvedt and Giordano found a significant correlation between water-soluble fractions of Zn and Zn availability to crops from several macronutrient fertilizers with zinc oxide (ZnO) or zinc sulfate incorporated.³ Further investigations have confirmed that water-soluble Zn, not the total Zn concentration, is the major parameter controlling the effectiveness of Zn-enriched fertilizers for plant growth and development.^{4–7}

Inorganic sources of Zn such as ZnO are among the most commonly used Zn fertilizers which have been globally applied to crops in Zn-deficient regions.⁸ Given that ZnO particles are sparingly soluble in water, incorporation of ZnO nanoparticles (ZnO NPs) into fertilizers as a source of Zn might be a promising approach which can exploit novel solubility features of ZnO NPs to improve the efficiency of Zn fertilizers.

In theory, the solubility of solids depends on the excess surface energy, which is correlated with the specific surface area and thus also with the particle size.⁹ According to the Ostwald–Freundlich

equation, the relative solubility of spherical particles of the same material increases as the particle size decreases in solid–liquid systems.¹⁰ On the basis of this relationship, the effect of particle size on solubility is more significant for particles with an equivalent spherical diameter of less than 0.1 μm .⁹ Furthermore, the dissolution kinetics of a particle, expressed by the Noyes–Whitney equation, suggest the dissolution rate of particles is directly proportional to their surface area because a relatively larger interface for dissolution is available, which promotes diffusion of dissolved ions away from the particles.^{10,11} On the basis of these thermodynamic and kinetic principles, ZnO NPs in soils should dissolve faster and to a greater extent than bulk ZnO particles (equivalent spherical diameter >100 nm). Consequently, application of ZnO NPs rather than bulk ZnO particles as a source of Zn in Zn fertilizers may improve the efficiency of the fertilizer and Zn availability to plants by enhancing the rate and extent of Zn dissolution.

Nevertheless, thermodynamically based considerations of nanoparticle dissolution have been challenged by some experimental results.^{12,13} Vogelsberger et al.¹³ reported a high dissolution rate of oxide nanoparticles at the beginning of the dissolution process when the saturation concentration was exceeded, followed by a decrease in the dissolution rate. A “self-inhibition”

Received: July 12, 2011

Revised: March 23, 2012

Accepted: April 5, 2012

Published: April 5, 2012

phenomenon was also proposed for sparingly soluble salts in which dissolution deceleration and eventually dissolution suppression were observed as the particle size of the dissolving crystals reached a critical nanoscale size. Therefore, high interfacial energy of the nanoparticles can dynamically stabilize the suspensions of nanosized particles.^{12,13} Although changes in the saturation state of the solution can restart nanoparticle dissolution,¹² aggregation of NPs needs to be considered when NPs are added into natural environments. Franklin et al.,⁴³ for instance, reported comparable dissolution rates and solubilities for nanoparticulate and bulk sources of ZnO due to aggregation in an algal growth medium. Moreover, the presence of plant roots and their exudates may further complicate the dissolution behavior of ZnO NPs. Therefore, it is critical to investigate the dissolution behavior of ZnO NPs in porous media without the presence of plants to develop a thorough mechanistic understanding of the dissolution of ZnO NPs in soils.

Coating of ZnO powders onto macronutrient fertilizer granules was selected as the preferred method of Zn inclusion into fertilizers. Incorporation or bulk blending of ZnO particles with macronutrient granules may result in chemical interactions or segregation of the Zn source, respectively.¹⁴ It is assumed that the coating process could minimize the reactions of Zn with phosphate in the monoammonium phosphate (MAP) treatments during incorporation or prevent Zn segregation which may occur during storage and handling of blended Zn compounds with macronutrient fertilizers. Therefore, the fertilizer grade can be maintained and a more uniform spread of Zn would be possible in the field with coated fertilizers. While application of Zn solutions is a common procedure in the coating process of fertilizers, the difficulty in maintaining a homogeneous dispersion of sparingly soluble ZnO particles during the coating process is a drawback. This is because it may result in a nonuniform distribution of Zn at the surface of the fertilizer granule and thus reduce the quality of the Zn-coated fertilizer. Hence, ZnO powders were applied in the coating process.

The dissolution behavior of ZnO NPs coated on macronutrient fertilizers and possible effects of macronutrient fertilizers on the dissolution behavior of ZnO NPs are important to understand before recommendation of the use of fertilizers containing ZnO NPs. Therefore, the aim of this study was to examine the solubility and dissolution (release) kinetics of Zn from ZnO NPs and bulk ZnO particles and from the same materials coated onto two commercial macronutrient fertilizers, urea and MAP. The dissolution behavior of Zn standard compounds was also investigated to provide information on possible mineral Zn phases controlling Zn dissolution. To the best of our knowledge, there is no literature on the solubility and dissolution rates of Zn from ZnO NPs coated onto macronutrient fertilizers. The information will be used as a first step in examining the applicability of using ZnO NPs coated onto the surface of macronutrient fertilizers to improve Zn fertilizer efficiency and availability to plants.

MATERIALS AND METHODS

Characterization of ZnO Particles. The ZnO NP powder (nominal diameter 20 nm, 99.5%) was purchased from Nanostructure & Amorphous Material Inc. (Houston, TX), and the bulk ZnO powder (nominal diameter <1 μm , 99.9%) was purchased from Sigma-Aldrich (Sydney, Australia). The ZnO particles did not contain surface capping agents or modifiers. The size and morphology of the particles were examined using transmission electron microscopy (TEM; Phillips

CM200, Eindhoven, The Netherlands) operating at 80 keV. A 100 mg L⁻¹ suspension of ZnO NPs was prepared in ultrapure deionized water (Milli-Q, Millipore, Billerica, MA) and sonicated for 3 min at 1500 W L⁻¹ using an ultrasonic probe (VirtisVirsonic, Gardiner, NY). The z-averaged hydrodynamic diameter and electrophoretic mobility of ZnO nanoparticles in the resulting suspension were determined using dynamic light scattering (DLS; Zetasizer Nano ZS, Malvern Instruments Ltd., United Kingdom), which allowed calculation of ζ potentials. X-ray diffraction (XRD) was used to identify Zn phases and to estimate the crystallite size of ZnO NP and bulk ZnO powders using the Sherrer equation. The XRD patterns were collected with a PANalytical X'Pert Pro microprocessor-controlled diffractometer (Almelo, The Netherlands) using Co K α radiation, an automatic divergence slit, a graphite postdiffraction monochromator, and a fast Si strip detector. The diffraction patterns were collected from $2\theta = 4^\circ$ to $2\theta = 80^\circ$ with a step size of $2\theta = 0.05^\circ$ and a 0.5 s counting time per step. The specific surface area of the particles was determined using the Brunauer–Emmett–Teller (BET) surface area equation¹⁵ after liquid N₂ adsorption (Quantachrome, Boynton Beach, FL).

Preparation of Coated Fertilizer Granules. Monoammonium phosphate (Mosaic Co., Plymouth, MN) and commercial urea fertilizer granules were sieved to obtain granules with diameters of 2000–3350 and 1676–2000 μm , respectively. Zinc oxide NPs or bulk ZnO particles were coated onto the surface of MAP or urea granules at a rate of ~1.5% Zn by weight. The granules and ZnO powder treatments were added to a Petri dish and then vigorously shaken manually. The mixtures were sprayed with a small amount of ultrapure deionized water using a 50 $\mu\text{L min}^{-1}$ nebulizer to provide a binding agent for the ZnO powders. Although the mixture of urea granules and ZnO is hygroscopic,¹⁶ a small amount of water was also sprayed onto this treatment to ensure complete coating of urea granules without dissolving them. Coated granules were air-dried at a relative humidity of approximately 30% in a laminar-flow cabinet. Adequate space was allocated to the coated granules to reduce contact of granules and possible caking.

The ZnO-coated MAP and urea granules were cross-sectioned manually using stainless steel blades. The cross-sectioned samples were coated with C and Au to reduce static electric charge accumulation and increase the signal intensity and resolution. The samples were mounted onto Al specimen holders for scanning electron microscopy (SEM) analysis using a Philips XL30 field emission scanning electron microscope (Eindhoven, The Netherlands) combined with an integrated energy-dispersive X-ray analysis (EDXA) Genesis EDX spectrometer system (EDAX, Mahwah, NJ) for elemental composition analysis. The SEM images of cross-sectioned granules as well as EDXA spectra on selected points of interest on the coating and inner parts of the fertilizer granules were collected at 20 keV.

Mineralogical characteristics of the coatings on the fertilizer granules were investigated using XRD. The coated fertilizer granules were milled to powders using a Spex shaker mill and ground in an agate mortar and pestle. The powders were lightly sprinkled onto silicate low-background holders for XRD analysis.

Total and Water-Soluble Zinc Concentrations of Coated Fertilizers. The total Zn concentrations of individual granules were determined using open vessel aqua regia extraction (9 mL of hydrochloric acid (HCl)/3 mL of nitric acid (HNO₃) at 140 °C followed by analysis of the digest solutions using inductively coupled plasma optical emission spectroscopy (ICP-OES; Spectro, Kleve, Germany).

Water-soluble Zn concentrations of coated granules were measured by agitating 0.5 g of each coated fertilizer granule in 30 mL of ultrapure deionized water (Millipore) for 24 h in an end-over-end shaker. The samples were then centrifuged for 20 min at 7000g and filtered using a syringe microfilter with a 0.22 μm particle size cutoff (Millipore, Ireland) and centrifugal ultrafiltration devices with a 1 kDa molecular mass cutoff (Pall Corp., Port Washington, NY) to differentiate dissolved and nanoparticulate Zn concentrations in the supernatants. Centrifugal 1 kDa filters (pore size ca. 1 nm)^{17,18} were used in this study to determine the dissolved <1 kDa fraction of Zn in suspensions and evaluate the efficiency of 0.22 μm filters in

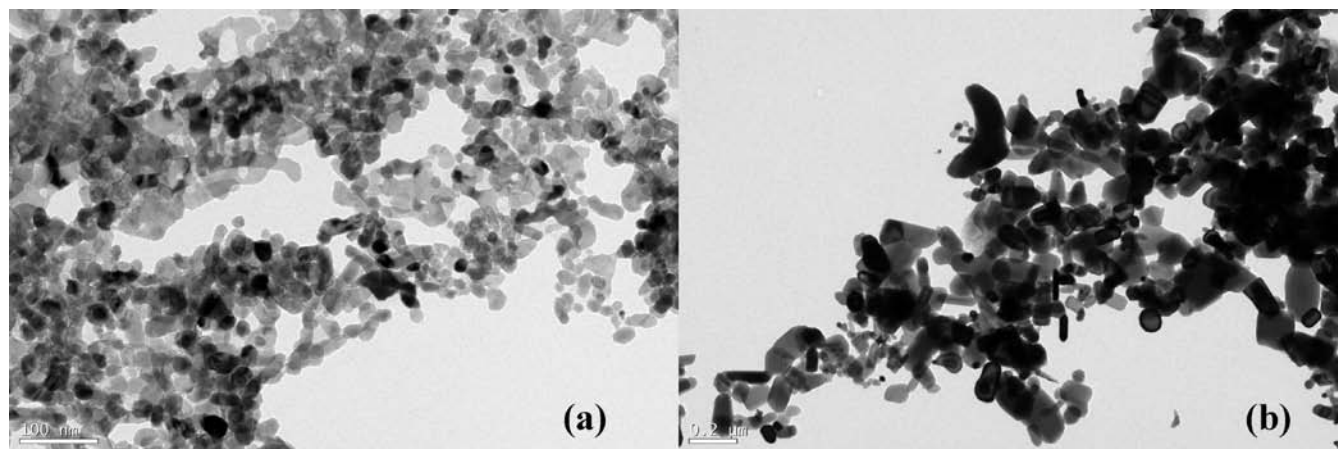


Figure 1. Transmission electron microscopy image of the ZnO powders used in the experiments: (a) ZnO NPs (nominal diameter of 20 nm), (b) bulk ZnO (nominal diameter <1 μm).

distinguishing “truly dissolved” Zn species from nanoparticulate ZnO. Zinc concentrations in 0.22 μm and 1 kDa filtrates were determined using ICP-OES.

Dissolution Kinetics of Zn from Coated Fertilizers. Dissolution kinetic experiments were conducted in sand columns instead of soil columns to eliminate the influence of soil on the dissolution kinetics of Zn from ZnO-coated fertilizers, but still provide a porous medium for dissolution. The experimental columns were constructed using polypropylene columns (150 mm \times 15 mm) and acid-washed sand (250–500 μm particle sizes). The specific and bulk densities of the sand were 2.64 and 1.58 g cm^{-3} , respectively. The columns were packed with 20 g of acid-washed sand. Then 1 g of coated fertilizer granules or a calculated amount of Zn standard compounds (equivalent to 15 mg of Zn per column) was placed on the surface of the sand, and an additional 10 g of sand was added to cover the fertilizer granules or Zn powders. Two polypropylene column caps were filled with a small amount of acid-washed glass wool and fitted to the top and bottom of each column to prevent disturbance and loss of sand during the experiment. The percolating solution (0.01 mol L^{-1} CaCl_2 , pH 4) was introduced using a peristaltic pump from the bottom of the sand column to maintain a constant flow rate of 10 mL h^{-1} . The solution at the top of the columns was collected every hour for 48 h using a fraction collector (SuperFracTM, Pharmacia). The solutions were 0.22 μm filtered as no significant difference between total Zn concentrations in <1 kDa and <0.22 μm filtrates was found during the Zn solubility study. Total Zn and P concentrations in each fraction were measured using ICP-OES. The solution pH was measured in all collected fractions. All treatments were replicated. Control columns containing only the acid-washed sand were analyzed throughout the study.

The dissolution kinetics of powdered ZnO NPs, powdered bulk ZnO, and standard Zn compounds were investigated. Standard Zn compounds examined were zinc phosphate ($\text{Zn}_3(\text{PO}_4)_2$) (Aldrich, 99.999%), zinc sulfate ($\text{ZnSO}_4 \cdot 7\text{H}_2\text{O}$) (AnalaR, 99.5%), and zinc carbonate hydroxide (hydrozincite, $\text{Zn}_5(\text{CO}_3)_2(\text{OH})_6$). Hydrozincite with a crystal size of approximately 14 nm was synthesized according to Zhang et al.,¹⁹ and the elemental composition was also confirmed by XRD.

Statistical Analysis and Thermodynamic Modeling. The variation in solubility of Zn from coated fertilizer granules in ultrapure water as well as variations in cumulative release of Zn from different treatments in sand columns were analyzed using a factorial experimental design with groups using the GENSTAT 13 package (VSN International Ltd., United Kingdom).

Thermodynamic modeling was carried out using Visual MINTEQ, version 2.60.²⁰ Equilibrium constants for all solid phases and aqueous species except $\text{Zn}(\text{NH}_4)\text{PO}_4$ were taken from the MINTEQ 4.0 database.²¹ The solubility constant of $\text{Zn}(\text{NH}_4)\text{PO}_4$ was calculated as $\log K_{\text{sp}} = -12.4$ (Degryse et al., personal communication). The effect

of the P concentration on the solubility of Zn from hopeite ($\text{Zn}_3(\text{PO}_4)_2 \cdot 4\text{H}_2\text{O}$) was modeled using the maximum and minimum concentrations of P (0.26 and 0.00013 mol L^{-1} PO_4^{3-} , respectively) detected in the fractions collected. All calculations were performed at 0.00038 atm of pressure for $\text{CO}_2(\text{g})$.

RESULTS AND DISCUSSION

Characterizations of ZnO NP and Bulk ZnO Powders.

The TEM image of ZnO NPs in a water suspension showed large aggregates of nearly spherical particles (Figure 1). The presence of aggregates of ZnO NPs may be due to sample preparation for TEM (air-drying) and/or aggregation of ZnO NPs in suspensions. The z-average hydrodynamic diameter of the aggregates of ZnO NPs in the suspension was estimated to be 312 nm. However, size estimates based on crystallite size with XRD and BET- N_2 analysis suggested a primary particle diameter for ZnO NPs consistent with the nominal particle size of ~ 20 nm (Table 1), which suggests a high degree of

Table 1. Selected Characteristics of the Manufactured ZnO NPs and Bulk ZnO Particles Used in the Experiments

property	ZnO nanoparticles	bulk ZnO
crystal structure	zincite	zincite
specific surface area (BET- N_2)	31 $\text{m}^2 \text{g}^{-1}$	12 $\text{m}^2 \text{g}^{-1}$
nominal particle diameter	20 nm	<1 μm
crystallite particle diameter (Scherrer equation estimate)	20 nm	100 nm
particle diameter (BET- N_2 estimate)	35 nm	88 nm

aggregation of ZnO NPs in water suspensions. Rapid aggregation of uncoated ZnO NPs into micrometer-scale aggregates in aqueous suspensions has been previously reported.²² Nanoparticles aggregate faster than bulk particles because the Brownian motion is faster and there are a larger number of particles for the same mass concentration, which increases the frequency of collisions leading to aggregation.²³

The ZnO NPs in this study had a relatively low surface charge of +15.7 mV in water, possibly because the pH (8) was close to the point of zero charge (pH_{pzc} 8.7–10.3²⁴) and the ionic strength of the ZnO suspension in 0.01 mol L^{-1} CaCl_2

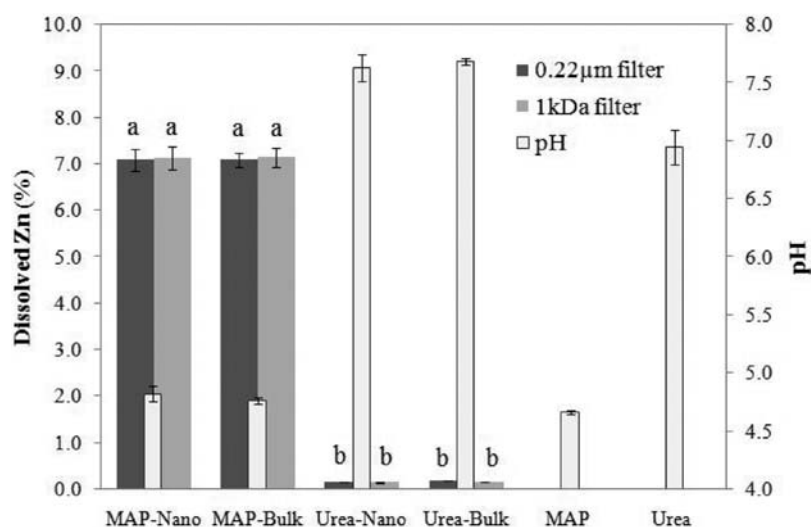


Figure 2. Batch water solubility of Zn from coated fertilizer granules (0.5 g in 30 mL, 24 h). The pH values of the suspensions are also shown as white bars.

was ca. 30 mmol L⁻¹, which is higher than the critical coagulation concentration of ZnO nanoparticles (0.125 mmol L⁻¹ CaCl₂).²⁵ A low surface charge and high ionic strength are conducive for nanoparticle aggregation.^{23,26,27}

The TEM images of aqueous suspensions of bulk ZnO (<1 μm) revealed large aggregates of particles with different sizes (Figure 1). The average crystallite size of bulk ZnO particles was 100 nm, and the specific surface area of 12 m² g⁻¹ corresponds to a diameter of 88 nm (Table 1). Particles much larger than 100 nm were observed in TEM images of bulk ZnO (Figure 1), and the specific surface area was larger than for ZnO NPs (Table 1). It can thus theoretically be expected that the bulk ZnO will be less soluble than the smaller ZnO nanoparticles. The XRD patterns indicated that ZnO NPs and bulk ZnO powders were primarily zincite (ZnO) (see the Supporting Information).

Characteristics of Coated Fertilizer Granules. The total Zn concentrations in coated urea and MAP fertilizers were ca. 1.5% by weight (see the Supporting Information). There was no significant difference in Zn concentrations between granules coated with bulk ZnO or ZnO NPs ($p \leq 0.05$). While soluble Zn usually reacts with ammonium orthophosphate to form Zn(NH₄)PO₄,^{28,29} our results indicate that Zn(NH₄)PO₄ also forms after reaction of ZnO powders with MAP granules. The SEM images of cross-sectioned fertilizers indicated a nearly homogeneous distribution of ZnO on the surface of the fertilizer granules, in the cases of both bulk ZnO and ZnO NPs (see the Supporting Information).

The EDXA spectra of ZnO-coated MAP granules confirmed that the inner granule contained mainly P, O, and N, while the elemental composition of the coating predominantly consisted of P, Zn, and O followed by N. The XRD analysis mainly detected Zn(NH₄)PO₄ and only a small amount of zincite (ZnO) (see the Supporting Information). This finding suggests that, during coating of MAP granules with ZnO powders, dissolution of ZnO occurred at acidic pH at the surface of MAP fertilizer granules and Zn precipitated as Zn(NH₄)PO₄.

In the case of urea granules, the Zn speciation was not altered by the coating. The EDXA spectra confirmed the presence of mainly Zn and O on the coatings of the granules, while the EDXA spectra from the inner granule area consisted of N, C,

and O. The XRD patterns indicated Zn was present as zincite at the surface of urea granules in the cases of both ZnO NPs and bulk ZnO. To evaluate possible regrowth of ZnO NPs to bulk ZnO particles at the surface of urea granules during the coating process, the crystallite size of ZnO NPs at the surface of urea granules was estimated using XRD patterns. The results showed that ZnO NPs at the coating of urea granules had a crystallite size (20–30 nm) similar to that of the original ZnO NPs.

Water Solubility of Zn from ZnO-Coated Fertilizers.

Coated MAP granules released significantly higher amounts of Zn compared to coated urea granules ($p < 0.001$) (Figure 2). The greater dissolution of Zn from MAP granules in water may be due to the greater acidity produced by MAP granules in solutions (pH 4.8) compared to the alkalinity produced by dissolution of urea granules (pH 7.6) (Figure 2). This confirms earlier work by Mortvedt and Giordano³ that showed ZnO granulated with urea was poorly water-soluble and also not effective in supplying Zn to corn in glasshouse experiments.

The solubilities of the two sources of ZnO powder (nanoparticulate and bulk) coated on MAP fertilizer granules did not differ significantly ($p = 0.849$) (Figure 2). Similar solubilities of two sources of ZnO may be because the Zn solubility was controlled by Zn(NH₄)PO₄ precipitation on the surface of MAP granules coated with either ZnO particle size. The solubilities of Zn from urea granules coated with ZnO NPs or bulk ZnO were not significantly different either ($p = 0.124$), although these particles appeared not to be chemically altered during coating. Zinc concentrations in <1 kDa (i.e., ionic Zn) and <0.22 μm (i.e., ionic zinc and ZnO NPs) filtrates of urea granule suspensions were not significantly different (Figure 2), which suggests that if ZnO NPs were released from the fertilizer coating, they formed aggregates larger than 0.22 μm. Urea granules undergo rapid hydrolysis in an aqueous suspension,³⁰ which explains the higher pH and reduced ZnO solubility relative to those of the more acidic MAP granules. In addition, Visual MINTEQ modeling showed that the ionic strength of the suspensions of urea granules was 500 mmol L⁻¹, which is much higher than the typical critical coagulation concentration of uncoated ZnO NPs (ca. 0.125 mmol L⁻¹).²⁵ Aggregation of any ZnO NPs that were released into the suspension would have been rapid. The dissolutions of

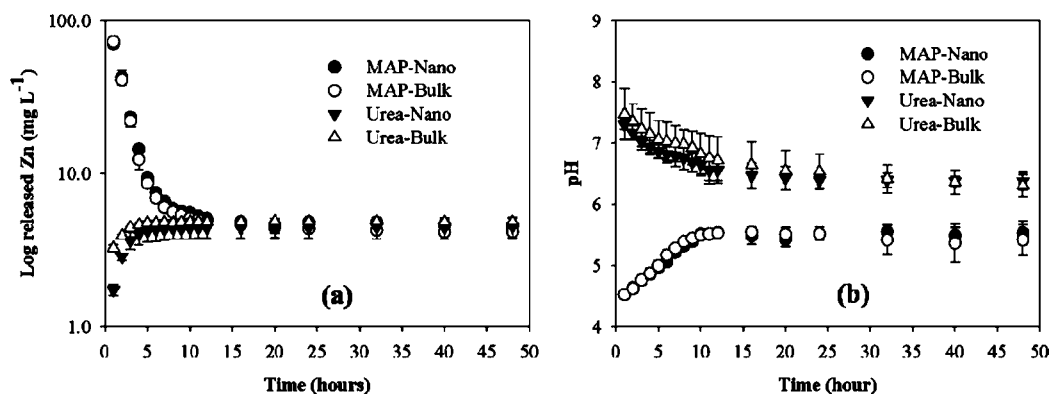


Figure 3. (a) Release of Zn from fertilizer granules coated with bulk ZnO or ZnO NPs. (b) Changes in the pH of the eluate from the columns.

aggregated ZnO NPs and bulk ZnO were therefore comparable, because of comparable surface areas and kinetic hindrance of Zn dissolution from ZnO aggregates. Moreover, because of aggregation, 0.22 μm filters were sufficient for separating ZnO NPs from dissolved Zn^{2+} ions.

Dissolution Kinetics of Zn from ZnO-Coated Fertilizers. The dissolution rate of ZnO NPs and bulk ZnO in coatings was dependent on the type of macronutrient fertilizer (Figure 3a). In the case of ZnO-coated MAP, Zn release increased rapidly for ca. 8 h, after which it decreased to a nearly constant value. In contrast, Zn release from both coated urea treatments increased slowly over time and reached a plateau after a few hours (Figure 3a). There was a significantly higher cumulative release of Zn from ZnO NPs and bulk ZnO coated on MAP (~20%) compared to urea granules (~15%) after 48 h ($p = 0.007$) (Table 2). The cumulative Zn release from bulk

MAP granules was initially much lower than that for urea granules (Figure 3b), which simulates the significant acidification effect that MAP granules have after application to different soils.³¹ However, the eluate pH from columns with MAP granules increased over time, which may be due to proton consumption during dissolution of Zn species from the surface of fertilizer granules.^{32,33}

In contrast, the pH of the initial fractions from columns with coated urea granules was 7.4, which decreased to pH 6.3 after 48 h (Figure 3b). Initial high pH values were likely due to the urea hydrolysis, which increased the pH of the eluate in the same manner as urea application enhanced the pH of soil microsites in an earlier study reported by Fan et al.³⁴ However, once dissolution of the urea granules was complete, the column eluate tended toward the pH values resulting from dissolution of ZnO. The initial reduced elution of Zn from coated urea granules may also be due to deposition of positively charged ZnO NPs and/or dissolved Zn species (Zn^{2+} , $\text{Zn}(\text{OH})^+$, aqueous $\text{Zn}(\text{OH})_2$, and ZnCl_2) at the surface of negatively charged sand particles in the columns (the point of zero charge for sand is approximately pH 2³⁵). A decline in the deposition rate of ZnO NPs due to the saturation of the sand surfaces³⁶ may be the reason for further enhancement of Zn elution from the columns, as this phenomenon has been reported for ZnO NP suspensions at a pH above 7 in clean quartz sand columns.³⁷ For both coated urea and MAP treatments, the pH of the eluate did not converge to the pH of the CaCl_2 solution (4) (Figure 3b). Moreover, the ionic activity products (IAPs) calculated for different treatments were much lower than the solubility constant reported for ZnO by Lindsay.³⁸ Accordingly, it can be inferred that, on the basis of solubility constants,³⁸ the system did not achieve equilibrium and the dissolution process continued in the undersaturated solutions (with respect to ZnO).³⁹

Table 2. Eluate pH for the First and Last Fractions Collected and Cumulative Release of Zn (Percentage of Zn Added to the Column) at the End of the Experimental Period (48 h)

treatment	pH value of the fractions collected		cumulative Zn released in 48 h (percentage of added Zn) ^a
	first fraction (1 h)	last fraction (48 h)	
MAP-nano-ZnO	4.5	5.5	22.8 a
MAP-bulk ZnO	4.5	5.4	20.2 a
urea-nano-ZnO	7.3	6.4	14.9 b
urea-bulk ZnO	7.5	6.3	15.4 b
nano-ZnO	6.9	6.4	16.2 b
bulk ZnO	6.5	6.4	16.4 b

^aDifferent lowercase letters indicate significant differences between rows.

ZnO and ZnO NPs coated on urea granules was comparable to that from bulk ZnO or ZnO NP powders alone (Table 2). This suggests that, in spite of the inhibitory effect of high pH generated by urea hydrolysis on ZnO dissolution in the first few fractions collected, the total dissolved Zn was not affected. This may be due to the removal of hydroxide or carbonate/bicarbonate ions generated through urea hydrolysis over time from the columns.

Differences in the release rate and cumulative Zn dissolution from coated MAP and urea treatments can be related to pH differences caused by dissolution of macronutrient fertilizer granules (Figure 3b). The pH of eluates from columns with

Although comparable Zn concentrations were collected from columns treated with coated MAP or urea in the final eluates (Figure 3a), the pH values of the eluates were different for these granules (Figure 3b). The differences in the pH value of the final eluates collected from coated MAP or urea suggest that different Zn minerals were controlling the Zn release from these coated products. Moreover, the steady-state concentrations achieved (i.e., $6.5 \times 10^{-5} \text{ mol L}^{-1}$) were much lower than estimations based on the solubility of ZnO or $\text{Zn}(\text{NH}_4)\text{PO}_4$ (e.g., $\sim 1.6 \times 10^{-4}$ and $2.3 \times 10^{-3} \text{ mol L}^{-1}$, respectively). Solubility diagrams were plotted using solution compositional data to predict possible Zn minerals controlling Zn solubility in our experimental systems (Figure 4). Two lines

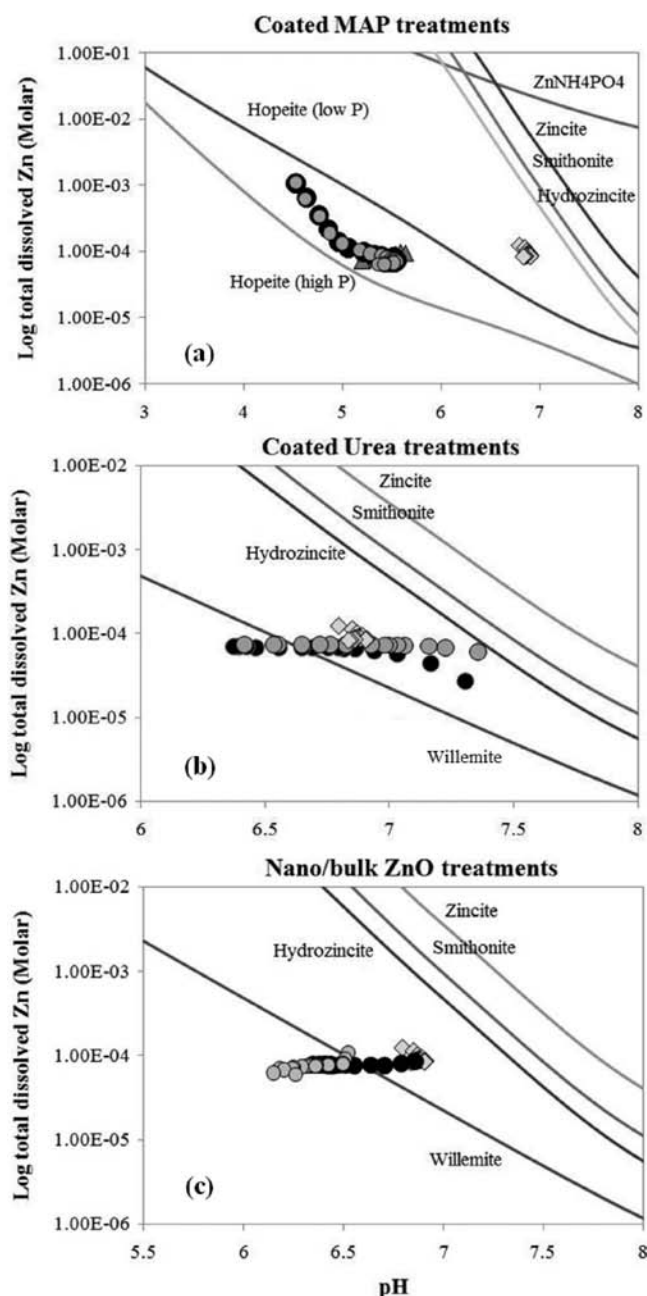


Figure 4. Solubility diagram of Zn minerals in the 0.01 mol L⁻¹ CaCl₂ solution and in equilibrium with atmospheric CO₂. The curves for hopeite (Zn₃(PO₄)₂·4H₂O) were plotted using Visual MINTEQ with respect to the highest (0.26 mol L⁻¹ PO₄²⁻) and lowest (0.00013 mol L⁻¹ PO₄²⁻) concentrations of P measured in the eluates. Results from the kinetics of dissolution were plotted on the solubility diagrams to evaluate the Zn mineral(s) possibly controlling Zn solubility. Black and gray circles represent treatments containing ZnO NP and bulk ZnO powders, respectively. Rhombus and triangle points illustrate the experimental results for ZnCO₃ and Zn₃(PO₄)₂ minerals, respectively. The area below the curves represents undersaturated conditions, and the area above the curves indicates supersaturated conditions.

were plotted for hopeite (Zn₃(PO₄)₂·4H₂O) to reflect the effect of different dissolved P concentrations. The position of experimental data from coated MAP granules in the phase diagram showed that the Zn dissolution in columns with coated MAP granules could have been controlled by hopeite

(Figure 4a), whereas Zn(NH₄)PO₄ was too soluble to control Zn dissolution. Figure 4b indicates zincite was too soluble to control Zn dissolution from urea granules. More likely, zinc carbonate-like species such as hydrozincite precipitated in the column with urea treatments. However, dissolved Zn²⁺ may have precipitated as a less soluble Zn mineral such as willemite (Zn₂SiO₄) over time. Our synchrotron-based investigations of coated urea granules incubated in a highly calcareous soil also revealed the presence of ZnCO₃-like minerals as a function of the distance from the point of application in the soil.⁴⁰ This supports the results of thermodynamic modeling which shows that hydrozincite is likely the main solid controlling the solubility of Zn from coated urea.

The results of Zn dissolution from columns with only ZnO (bulk/NPs) powders or ZnCO₃ are also plotted in the solubility diagram (Figure 4). On the basis of the positions of plotted experimental data, we hypothesize that the solubility of Zn is mainly controlled by hydrozincite in the first few eluates followed by willemite in the final eluates with lower pH. Insoluble sources of solid phases will need a long time for reactions with the solution to reach equilibrium,⁴¹ which might explain incomplete overlap of calculated equilibrium curves and experimental data.

The dissolution kinetics of Zn from coated fertilizer granules or from ZnO powders were not affected by the size of the ZnO particles (Figures 3a and 5a). The lack of any difference between MAP coated with ZnO NPs and bulk ZnO may be due to the unavoidable formation of Zn(NH₄)PO₄ species on the surface of MAP granules from the dissolution of ZnO in both treatments, either during the coating process or during the initial dissolution of the granule. The kinetics of Zn release from columns treated with ZnO NP powder or coated urea granules with ZnO NPs did not support the kinetic size model for nanoparticles, an observation that suggests very high dissolution rates at the beginning of the dissolution and further suppression of the release rate over time.^{12,13} The possible explanations could be an inhibitive effect of urea granules on the dissolution rate of ZnO in columns treated with coated urea granules and deposition of positively charged ZnO NPs and dissolved Zn species at the pH of the eluates onto negatively charged sand surfaces which concealed expected high initial dissolution or aggregation of ZnO NPs released to the eluted solution. Size-independent release of Zn from coated urea granules or ZnO powders can be explained on the basis of the solubility of the same compounds formed, irrespective of the size of the original ZnO particles. Comparable time-dependent solubilities of bulk and nanoparticulate sources of ZnO have been reported in different media in toxicological studies, resulting in similar toxicities for bulk and nanoparticulate sources of ZnO.⁴²⁻⁴⁵

Despite the traditional models that suggest greater and faster dissolution for nanoparticles compared to larger particles, our experimental results showed comparable solubilities for both sources of ZnO particles (which did not contain surface modifiers). We therefore observed little potential to markedly increase Zn fertilizer efficiency by using nanoparticulate sources of ZnO when Zn is coapplied with urea and MAP fertilizer granules. Given that the surface chemistry of nanoparticles can be greatly affected by capping agents such as surface coatings or functional groups, further investigations on the impact of surface modifications in improving the fertilizer formulation are a critical research need.

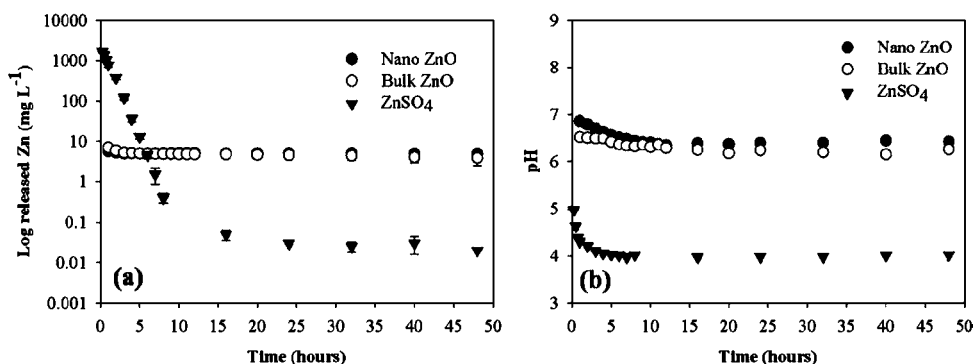


Figure 5. (a) Release of Zn from columns treated with bulk ZnO or ZnO NPs and ZnSO₄. (b) Changes in the pH of eluate solutions from the columns incubated with ZnO (bulk or nanoparticulate) and ZnSO₄ powders during the dissolution experiment.

■ ASSOCIATED CONTENT

Supporting Information

Additional details of the materials, including XRD patterns, SEM images, and Zn content of coated fertilizer granules, and additional figures on cumulative Zn release and dissolution kinetics of coated fertilizers, ZnO particles, and Zn standards. This material is available free of charge via Internet at <http://pubs.acs.org>.

■ AUTHOR INFORMATION

Corresponding Author

*E-mail: narges.milani@adelaide.edu.au. Phone: +61(08) 83037284. Fax: +61(08) 83036511.

Present Addresses

^{||}National Risk Management Research Laboratory, U.S. Environmental Protection Agency, 919 Kerr Research Dr., Ada, OK.

[†]Chemistry Department, University of Gothenburg, Kemivägen 10, 41296 Gothenburg, Sweden.

Funding

A part of this project was conducted with financial support from the Nanosafety Theme, Advanced Materials Transformational Capability Platform, CSIRO.

Notes

The U.S. EPA has not subjected this manuscript to internal policy review. Therefore, the research results presented herein do not necessarily reflect Agency policy. Mention of trade names of commercial products and companies does not constitute endorsement or recommendation for use.

The authors declare no competing financial interest.

■ ACKNOWLEDGMENTS

We thank Dr. Peter Self for his help in TEM-EDXA and SEM-EDXA imaging and analysis, Mark Raven for XRD analysis, Lester Smith for his help in constructing sand columns and BET-N₂ analysis, and Claire Wright and Waite Analytical Services (WAS) for ICP-OES analysis. We appreciate the invaluable advice of Dr. Fien Degryse.

■ ABBREVIATIONS USED

DLS, dynamic light scattering; EDAX, energy-dispersive X-ray analysis; ICP-OES, inductively coupled plasma optical emission spectrometry; kDa, kilodalton; MAP, monoammonium phosphate; NPs, nanoparticles; SEM, scanning electron microscopy; TEM, transmission electron microscopy; XRD,

X-ray diffraction; ZnNH₄PO₄, zinc ammonium phosphate; ZnO, zinc oxide; ZnSO₄, zinc sulfate

■ REFERENCES

- (1) Sillanpaa, M. *Micronutrients and the Nutrient Status of Soils: A Global Study*; Food and Agriculture Organization of the United Nations (FAO): Rome, 1982; p 444.
- (2) Sillanpaa, M. *Micronutrient Assessment at Country Level: An International Study*; FAO: Rome, 1990; p 208.
- (3) Mortvedt, J. J.; Giordano, P. M. Extractability of zinc granulated with macronutrient fertilizers in relation to its agronomic effectiveness. *J. Agric. Food Chem.* **1969**, *17*, 1272–1275.
- (4) Amrani, M.; Westfall, D. G.; Peterson, G. A. Influence of water solubility of granular zinc fertilizers on plant uptake and growth. *J. Plant Nutr.* **1999**, *22*, 1815–1827.
- (5) Gangloff, W. J.; Westfall, D. G.; Peterson, G. A.; Mortvedt, J. J. Relative availability coefficients of organic and inorganic Zn fertilizers. *J. Plant Nutr.* **2002**, *25*, 259–273.
- (6) Shaver, T. M.; Westfall, D. G.; Ronaghi, M. Zinc fertilizer solubility and its effects on zinc bioavailability over time. *J. Plant Nutr.* **2007**, *30*, 123–133.
- (7) Westfall, D. G.; Mortvedt, J. J.; Peterson, G. A.; Gangloff, W. J. Efficient and environmentally safe use of micronutrients in agriculture. *Commun. Soil Sci. Plant Anal.* **2005**, *36*, 169–182.
- (8) Martens, D. C.; Westermann, D. T. Fertilizer applications for correcting micronutrient deficiencies. In *Micronutrients in Agriculture*; Mortvedt, J. J., Cox, F. R., Shuman, L. M., Welch, R. M., Eds.; Soil Science Society of America: Madison, WI, 1991; pp 549–592.
- (9) Stumm, W.; Morgan, J. J. *Aquatic Chemistry: Chemical Equilibria and Rates in Natural Waters*, 3rd ed.; Wiley: New York, 1996.
- (10) Borm, P.; Klaessig, F. C.; Landry, T. D.; Moudgil, B.; Pauluhn, J.; Thomas, K.; Trottier, R.; Wood, S. Research strategies for safety evaluation of nanomaterials, part V: Role of dissolution in biological fate and effects of nanoscale particles. *Toxicol. Sci.* **2006**, *90*, 23–32.
- (11) Sasson, Y.; Levy-Ruso, G.; Toledano, O.; Ishaaya, I. *Nano-suspensions: Emerging Novel Agrochemical Formulations*; Springer-Verlag: Berlin, 2007; pp 1–304.
- (12) Tang, R.; Orme, C. A.; Nancollas, G. H. Dissolution of crystallites: Surface energetic control and size effects. *ChemPhysChem* **2004**, *5*, 688–696.
- (13) Vogelsberger, W.; Schmidt, J.; Roelofs, F. Dissolution kinetics of oxidic nanoparticles: The observation of an unusual behaviour. *Colloids Surf., A* **2008**, *324*, 51–57.
- (14) Mortvedt, J. J.; Gilkes, R. J. Zinc fertilizers. In *Zinc in Soils and Plants*; Robson, A. D., Ed.; Kluwer Academic Publishers: Dordrecht, The Netherlands, Boston, MA, 1993.
- (15) Brunauer, S.; Emmett, P. H.; Teller, E. Adsorption of gases in multimolecular layers. *J. Am. Chem. Soc.* **1938**, *60*, 309–319.
- (16) Werner, E. A. Urea as a hygroscopic substance. *Nature* **1937**, *139*, 512.

- (17) Guo, L.; Santschi, P. H. Ultrafiltration and its application to sampling and characterization of aquatic colloids. In *Environmental Colloids and Particles: Behaviour, Separation, and Characterisation*; Wilkinson, K. J., Lead, J. R., Eds.; John Wiley: Chichester, U.K., 2007; pp 160–221.
- (18) Cornelis, G.; Kirby, J. K.; Beak, D.; Chittleborough, D.; McLaughlin, M. J. A method for determination of retention of silver and cerium oxide manufactured nanoparticles in soils. *Environ. Chem.* **2010**, *7*, 298–308.
- (19) Zhang, S.; Fortier, H.; Dahn, J. R. Characterization of zinc carbonate hydroxides synthesized by precipitation from zinc acetate and potassium carbonate solutions. *Mater. Res. Bull.* **2004**, *39*, 1939–1948.
- (20) Gustafsson, J. P. Visual MINTEQ, version 2.60, 2009. <http://www.lwr.kth.se/English/OurSoftware/vminteq/>. (Accessed May 2009).
- (21) Allison, J. D.; Brown, D. S.; Novo-Gradac, K. J. *MINTEQA2/PRODEFA2, a Geochemical Assessment Model for Environmental Systems: Version 3.0 User's Manual*; U.S. Environmental Protection Agency: Washington, DC, 1991.
- (22) Tso, C.; Zhung, C.; Shih, Y.; Tseng, Y.; Wu, S.; Doong, R. Stability of metal oxide nanoparticles in aqueous solutions. *Water Sci. Technol.* **2010**, *61*, 127–133.
- (23) Handy, R. D.; von der Kammer, F.; Lead, J. R.; Hasselov, M.; Owen, R.; Crane, M. The ecotoxicology and chemistry of manufactured nanoparticles. *Ecotoxicology* **2008**, *17*, 287–314.
- (24) Kosmulski, M. *Chemical Properties of Material Surfaces*; Marcel Dekker: New York, 2001.
- (25) Shih, Y.-h.; Wu, S. C.; Doong, R. A. The fate and transformation of nanoparticles in water environmental media. http://ehs.epa.gov.tw/Projects/EN_F_ResearchPrjs_Detail/1014. (Accessed February 2011).
- (26) Kallay, N.; Zalac, S. Stability of nanodispersions: A model for kinetics of aggregation of nanoparticles. *J. Colloid Interface Sci.* **2002**, *253*, 70–76.
- (27) Zhou, D.; Keller, A. A. Role of morphology in the aggregation kinetics of ZnO nanoparticles. *Water Res.* **2010**, *44*, 2948–2956.
- (28) Frazier, A. W.; Smith, J. P.; Lehr, J. R. Precipitated impurities in fertilizers prepared from wet-process phosphoric acid. *J. Agric. Food Chem.* **1966**, *14*, 522–529.
- (29) Hossner, L. R.; Blanchar, R. W. The utilization of applied zinc as affected by pH and pyrophosphate content of ammonium phosphates. *Soil Sci. Soc. Am. Proc.* **1969**, *33*, 618–621.
- (30) Gould, W. D.; Hagedorn, C.; McCready, R. G. L. Urea transformations and fertilizer efficiency in soil. In *Advances in Agronomy*; Brady, N. C., Ed.; Academic Press: New York, 1986; Vol. 40, pp 209–238.
- (31) Hettiarachchi, G.; Lombi, E.; McLaughlin, M.; Chittleborough, D.; Johnston, C. Chemical behavior of fluid and granular Mn and Zn fertilisers in alkaline soils. *Aust. J. Soil Res.* **2010**, *48*, 238–247.
- (32) Bian, S. W.; Mudunkotuwa, I. A.; Rupasinghe, T.; Grassian, V. H. Aggregation and dissolution of 4 nm ZnO nanoparticles in aqueous environments: Influence of pH, ionic strength, size, and adsorption of humic acid. *Langmuir* **2011**, *27*, 6059–6068.
- (33) Degen, A.; Kosec, M. Effect of pH and impurities on the surface charge of zinc oxide in aqueous solution. *J. Eur. Ceram. Soc.* **2000**, *20*, 667–673.
- (34) Fan, M. X.; Mackenzie, A. F. Urea and phosphate interactions in fertilizer microsites—Ammonia volatilization and pH changes. *Soil Sci. Soc. Am. J.* **1993**, *57*, 839–845.
- (35) He, F.; Zhang, M.; Qian, T. W.; Zhao, D. Y. Transport of carboxymethyl cellulose stabilized iron nanoparticles in porous media: Column experiments and modeling. *J. Colloid Interface Sci.* **2009**, *334*, 96–102.
- (36) Ryan, J. N.; Elimelech, M. Colloid mobilization and transport in groundwater. *Colloids Surf, A* **1996**, *107*, 1–56.
- (37) Kanel, S. R.; Al-Abed, S. R. Influence of pH on the transport of nanoscale zinc oxide in saturated porous media. *J. Nanopart. Res.* **2011**, *13*, 4035–4047.
- (38) Lindsay, W. L. *Chemical Equilibria in Soils*; Wiley, Inc.: New York, 1979.
- (39) Sparks, D. L. *Environmental Soil Chemistry*, 2nd ed.; Academic Press: Boston, MA, 2003.
- (40) Milani, N.; Hettiarachchi, G. M.; Beak, D. G.; McLaughlin, M. J.; Kirby, J. K.; Stacey, S. P. Fate of nanoparticulate zinc oxide fertilizers in an alkaline calcareous soil. *Soil Sci. Soc. Am. J.* **2012**, submitted for publication.
- (41) Robarge, W. P. Precipitation/dissolution reactions in soils. In *Soil Physical Chemistry*, 2nd ed.; Sparks, D. L., Ed.; CRC Press LLC: Boca Raton, FL, 1998.
- (42) Kasemets, K.; Ivask, A.; Dubourguier, H.-C.; Kahru, A. Toxicity of nanoparticles of ZnO, CuO and TiO₂ to yeast *Saccharomyces cerevisiae*. *Toxicol. Vitro* **2009**, *23*, 1116–1122.
- (43) Franklin, N. M.; Rogers, N. J.; Apte, S. C.; Batley, G. E.; Gadd, G. E.; Casey, P. S. Comparative toxicity of nanoparticulate ZnO, bulk ZnO, and ZnCl₂ to a freshwater microalga (*Pseudokirchneriella subcapitata*): The importance of particle solubility. *Environ. Sci. Technol.* **2007**, *41*, 8484–8490.
- (44) Wang, H.; Wick, R. L.; Xing, B. Toxicity of nanoparticulate and bulk ZnO, Al₂O₃ and TiO₂ to the nematode *Caenorhabditis elegans*. *Environ. Pollut.* **2009**, *157*, 1171–1177.
- (45) Li, M.; Zhu, L. Z.; Lin, D. H. Toxicity of ZnO nanoparticles to *Escherichia coli*: Mechanism and the influence of medium components. *Environ. Sci. Technol.* **2011**, *45*, 1977–1983.